JOURNAL OF GEOPHYSICAL RESEARCH, VOL. 102, NO. B6, PAGES 11,913-11,929, JUNE 10, 1997

Extension across a divergent plate boundary, the Eastern Volcanic Rift Zone, south Iceland, 1967-1994, observed with GPS and electronic distance measurements

Sigurjón Jónsson[1]
Science Institute and Physics Department, University of Iceland, Reykjavík

Páll Einarsson
Science Institute, University of Iceland, Reykjavík

Freysteinn Sigmundsson
Nordic Volcanological Institute, Reykjavík, Iceland

Abstract. The average spreading rate in south Iceland, 19 mm/yr, is distributed over two parallel rift zones. We measured a Global Positioning System (GPS) network of 42 stations in the eastern zone in 1994. This network consists of stations measured with GPS in 1986 and 1992, stations in a 60 km long distance profile measured several times since 1967, and a few new stations. The 1994 GPS data were processed using the Bernese software version 3.5, and the average position uncertainties are about 3 mm in horizontal components and about 8 mm in the vertical component for baselines up to 100 km. Comparison with results of former GPS campaigns gives a uniform extension, steady in time, perpendicular to the spreading axis. A strain rate of 0.12 ± 0.01 μstrain/yr is observed across the 100 km wide network, or an extension of about 12 mm/yr. Minor deformation is observed in direction parallel to the spreading axis. Observations along the distance profile, which lies across the rift zone, gave a significant contraction during the period 1967-1977 but gave an extension during 1977-1994. This extension is about 138 ± 47 mm and is mainly accommodated in the western part of the profile. The observed extension across the rift zone during 1986-1994 can be simulated with a simple model of infinitely long dike intrusions into an elastic layer overlying a viscous layer. This model is not able to simulate observed contraction along the distance profile 1967-1977. The observed irregularities along the western part of the distance profile coincide in space and time with volcanic and tectonic unrest near the Hekla volcano. The disturbances are probably caused by some common underlying process leading to crustal deformation, eruptions, and earthquakes.

Introduction

Volcanic and seismic zones form the Mid-Atlantic plate boundary in Iceland. The Mid-Atlantic Ridge (MAR) connects to the Reykjanes Peninsula in southwest Iceland. Spreading in the south part of Iceland occurs in two separate and parallel zones, known as the Western and the Eastern Volcanic Zone (WVZ and EVZ). These zones are connected by a transform zone, called the South Iceland Seismic Zone (SISZ). The Northern Volcanic Zone (NVZ) is a northward extension of the EVZ. It emanates from the Vatnajökull ice cap in the south and extends to the coast in the north, where the plate boundary is again connected to the MAR by the Tjörnes fracture zone (Figure 1a).

The EVZ extends from the Bárdarbunga and Grímsvötn central volcanoes (within the Vatnajökull glacier) in the northeast to the Vestmannaeyjar central volcano in the southwest (Figure 1). The EVZ is divided into two parts, north and south of its junction with the SISZ (Figure 1b). The part to the north has been called the Eastern Volcanic Rift Zone (EVRZ), but the part to the south has been called the Eastern Volcanic Flank Zone (EVFZ). *Jakobsson* [1972] found that during postglacial time the EVZ has emitted either tholeiitic or transitional to alkalic lavas. The former have been erupted along the rift zone, in the northern part, where rift structures are exposed. The latter have been erupted in the flank zone, in the southern part, where spreading seems to be negligible.

The EVRZ is structurally characterized by fissure swarms and palagonite ridges, with an orientation of about N45°E, emanating from the Vatnaj¨kull ice cap in the northeast toward the Torfajökull and Katla central volcanoes in the southwest [*Einarsson,* 1991]. At

[1]Now at Nordic Volcanological Institute and Iceland Geodetic Survey, Reykjavík, Iceland.

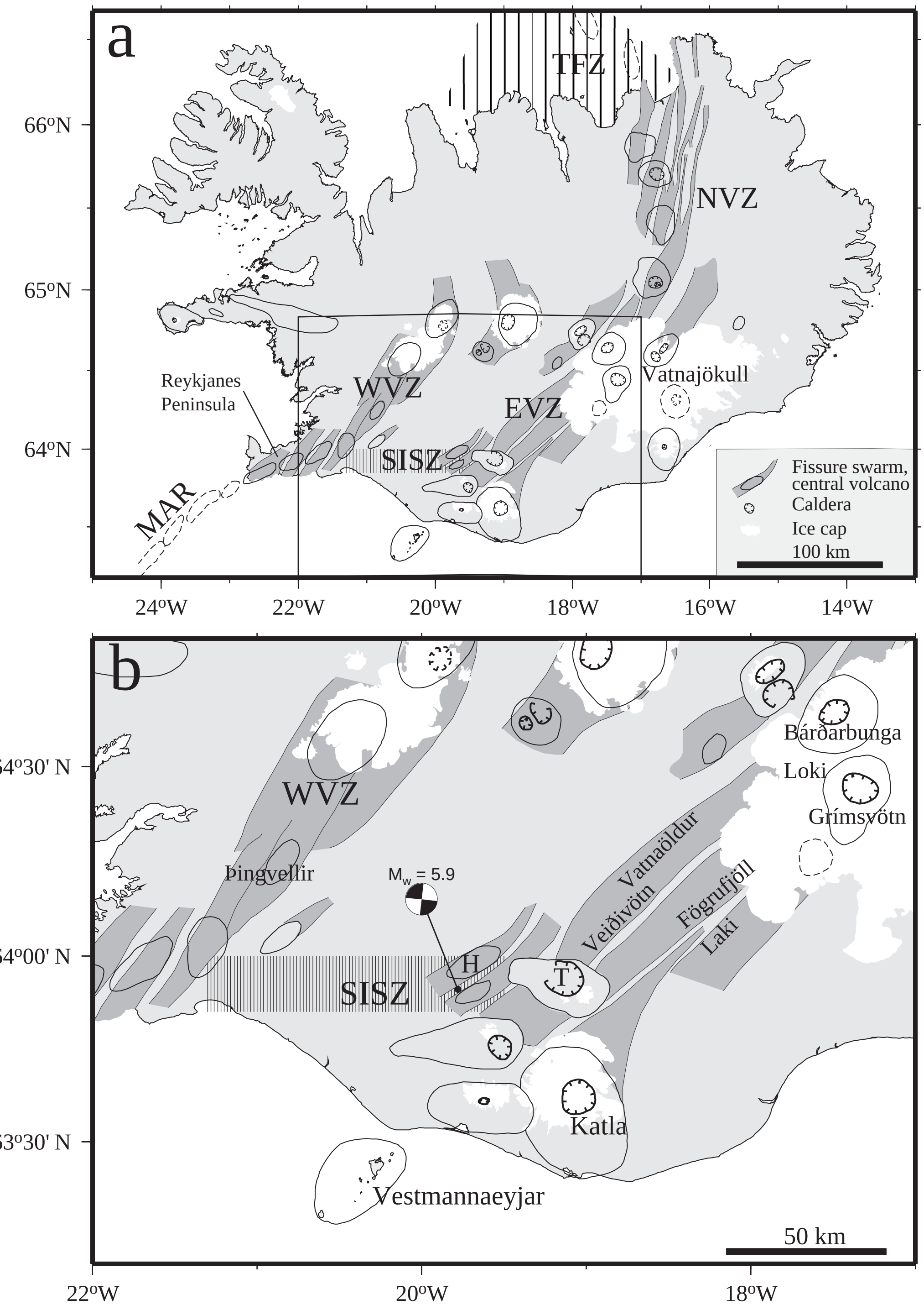

Figure 1: (a) The neovolcanic zones in Iceland. MAR, Mid-Atlantic Ridge; WVZ, Western Volcanic Zone; SISZ, South Iceland Seismic Zone; EVZ, Eastern Volcanic Zone; NVZ, Northern Volcanic Zone; TFZ, Tjörnes Fracture Zone. After *Einarsson and Sæmundsson* [1987]. (b) The EVZ, fissure swarms, central volcanoes and calderas. H and T denote the Hekla and Torfajökull central volcanoes. Focal mechanism and location of the 1987 Vatnafjöll earthquake are from *Bjarnason and Einarsson* [1991].

least two volcanic systems are in this rift zone, the Bárdarbunga central volcano and fissure swarm, including the Vatnaöldur and Veidivötn fissures, and the Grímsvötn central volcano and fissure swarm, including the Laki fissure. It has been argued, by evidence from radio echo soundings, earthquakes, and jökulhlaups (a sudden burst of water from a glacier caused by volcanic eruption or by draining of a water reservoir), that the third volcanic system exists between the systems of Bárdarbunga and Grímsvötn. It has been called the Loki volcanic system, and it may include the Fögrufjöll fissure swarm (Figure 1b) [*Björnsson and Einarsson,* 1990]. Seven volcanic systems were identified within the EVFZ by *Jakobsson* [1979], each having its own characteristic petrology, rock chemistry, and structural development. Present seismic activity in the EVZ is mainly related to the central volcanoes. The fissure swarms have been largely aseismic for the last decades [*Einarsson,* 1991]. The largest seismic event in the EVZ for the last 80 years was the Vatnafjöll earthquake in 1987, $M_w = 5.9$, near the Vatnafjöll central volcano (Figure 1b).

The global plate motions averaged over the last few million years indicate that the spreading rate in Iceland is about 19 mm/yr in the direction of N104°E, according to the NUVEL-1A model [*DeMets et al.,* 1994]. The WVZ seems to have been the only active zone in south Iceland from about 7 Ma to about 2 Ma [*Sæmundsson,* 1979], and it presumably accommodated all the spreading during that period. Since the opening of the EVZ, about 2 m.y. ago [*Sæmundsson,* 1979], these two parallel spreading zones have been active in south Iceland. It has been suggested that the EVZ has been propagating to the south and that it seems to be taking over as the main spreading center in south Iceland, while the WVZ appears to be a dying rift [*Einarsson,* 1991]. The main argument for this suggestion is the existence of the SISZ, which connects the EVZ to the southern tip of the WVZ. It is also noticeable that no volcanic activity has taken place in the WVZ during the last 2000 years, while several major rifting episodes have occurred in the EVZ.

The SISZ takes up the transform motion between the Reykjanes Peninsula and the EVZ. Instead of one large, east-west oriented transform fault, similar to those which exist elsewhere on the MAR, the SISZ accommodates the transform motion along many parallel, north-south, right-lateral faults and counterclockwise rotation of the blocks between them, that is, by bookshelf faulting [*Einarsson and Eiríksson,* 1982]. No similar transform zone is found near the north end of the WVZ indicating that the average spreading of 19 mm/yr in south Iceland cannot be evenly divided between the WVZ and EVZ at the present time.

There has been considerable rifting in the WVZ during the postglacial period, however, leading to a clear graben subsidence. Measurements in the Thingvellir area (within the southern part of the WVZ) show that cumulative width of fractures across the zone, exposed in 9000 years old lava, is about 100 m [*Gudmundsson,* 1987]. This corresponds to roughly half of the average total spreading in south Iceland. On the other hand, *Gudmundsson* [1987] mentioned that many of the large fractures of the Thingvellir swarm are of graben-like structure, and consequently, the true total dilatation of the Thingvellir swarm may be significantly less than the combined width of the fractures at the surface, that is, significantly less than 100 m. Furthermore, fractures and grabens are not clearly exposed 20-30 km north of the Thingvellir area (the same 9000 years old lava field), indicating that measured dilatation at Thingvellir is not representative for the average dilatation along the entire WVZ.

Over the period 1986-1992, *Sigmundsson et al.* [1995] observed little internal deformation in the area west of the WVZ (within the North American plate) and at the southern tip of the EVZ (within the Eurasian plate). The observed relative velocity of these two areas is 21 ± 4 mm/yr, and it is compatible with the predicted NUVEL-1A velocity of 19 mm/yr for this area [*DeMets et al.,* 1994]. The 1992 campaign did not fully cover the EVRZ, and it is not possible to see significant deformation across the zone from the results. *Sigmundsson et al.* [1995] observed that the area north of the SISZ moves to the west with the North American plate and the area to the south of the seismic zone moves to the east with the Eurasian plate. Their Global Positioning System (GPS) measurements indicate that about 85±15% of the relative plate motion during the 3 year period, 1989-1992 is accommodated by the seismic zone. They concluded that only 15±15% of the plate divergence is currently focused on the WVZ, and 85±15% of the plate divergence occurs in the EVZ.

GPS Geodesy in the EVRZ

The 1986 Survey

The first GPS measurements in Iceland were made in July 1986. *Foulger et al.* [1993] measured eight GPS stations in the EVRZ as a part of this country-wide campaign of 51 stations (Figure 2a). Five TI-4100 receivers were used. They observed two daily windows, a 2 hour 40 min long morning session and a 3 hour 20 min long evening session. Three or more satellites were visible above 10° during these sessions.

The data were processed using the Bernese software version 3 [*Rothacher et al.,* 1993]. The best solutions obtained were an ambiguity fixed L3 ionosphere-free solution for stations in south Iceland (short baselines) and ambiguity-free L3 solution for the country-wide network (long baselines). By studying the repeatability, *Foulger et al.* [1993] concluded that the solution for south Iceland is accurate to about 10-20 mm in horizontal position and 20-30 mm in height. For stations in the EVRZ in particular, the average position uncertainties were estimated to be 12, 11, and 23 mm, for the north, east, and vertical components, respectively (G. R. Foulger, personal communication, 1995).

The 1992 Survey

In July and August 1992, *Sigmundsson et al.* [1995] measured eight GPS stations in the EVRZ as a part of a campaign in south Iceland when 41 stations were occupied (Figure 2b). They used five Trimble 4000 SST receivers. The data recording interval was 15 s, and all visible satellites above 10° elevation were tracked [*Sigmundsson et al.,* 1992b]. Two sessions were observed every day, about 9 hour 30 min long day session and about 14 hour 30 min long night session. Each station was occupied for approximately four sessions, but there was just one antenna setup for each site.

The data were analyzed with version 3.3 of the Bernese GPS software. Two sets of coordinates were produced, one using broadcast orbit information and another using precise orbits from the International GPS Service for geodynamics (IGS) [*Beutler et al.,* 1994]. In the preferred solution, using IGS orbits, the average session-to-session

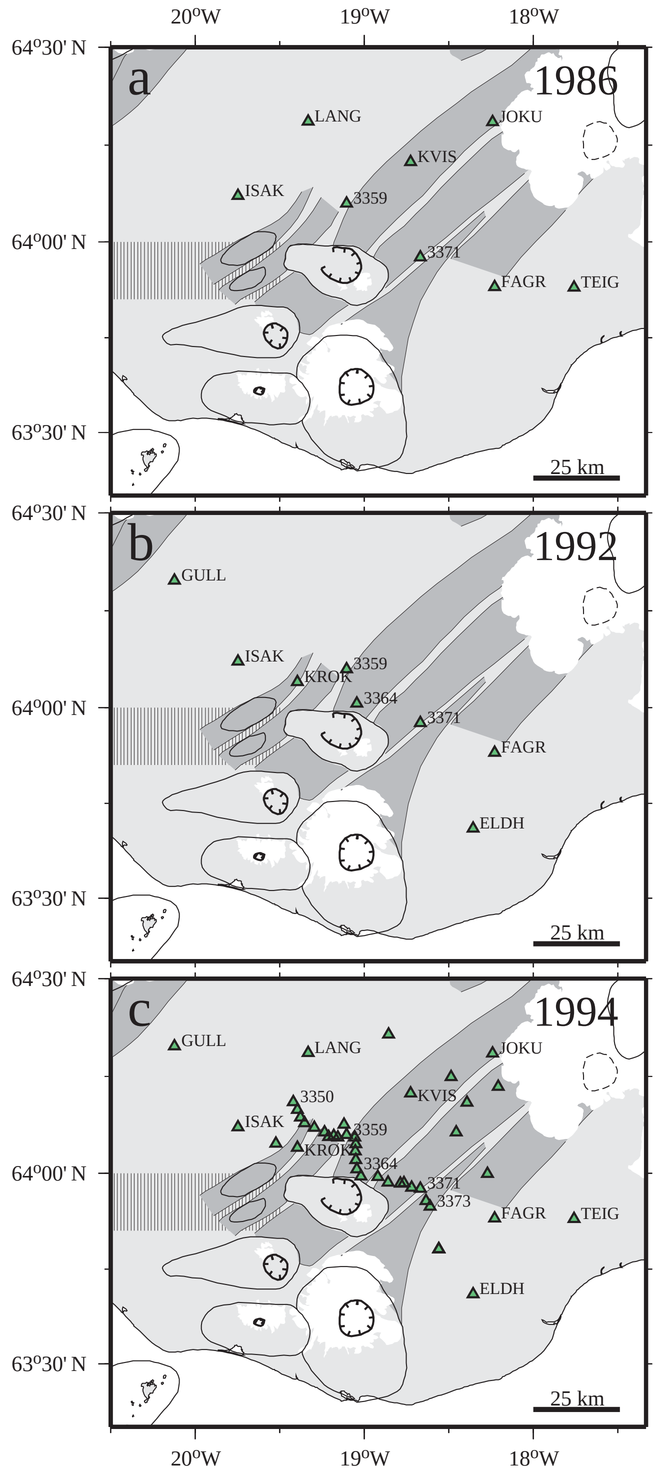

Figure 2: Global Positioning System (GPS) stations in the EVRZ measured in (a) 1986, (b) 1992, and (c) 1994. The station ISAK was used as a reference station during the surveys. A distance measurement profile, consisting of 24 bench marks, was measured for the first time using GPS in 1994 (between stations 3350 and 3373).

scatters were 2.7, 2.0, and 11 mm in the north, east, and vertical components, respectively. Including a 2 mm uncertainty for antenna setup, *Sigmundsson et al.* [1995] estimated the uncertainty of horizontal positions to be about 4 mm.

The 1994 Survey

In July to September 1994, we conducted the largest GPS campaign in the EVRZ so far, a network of 42 points was measured (Figure 2c). We remeasured stations that were measured in 1986 and 1992. A distance profile of 24 points

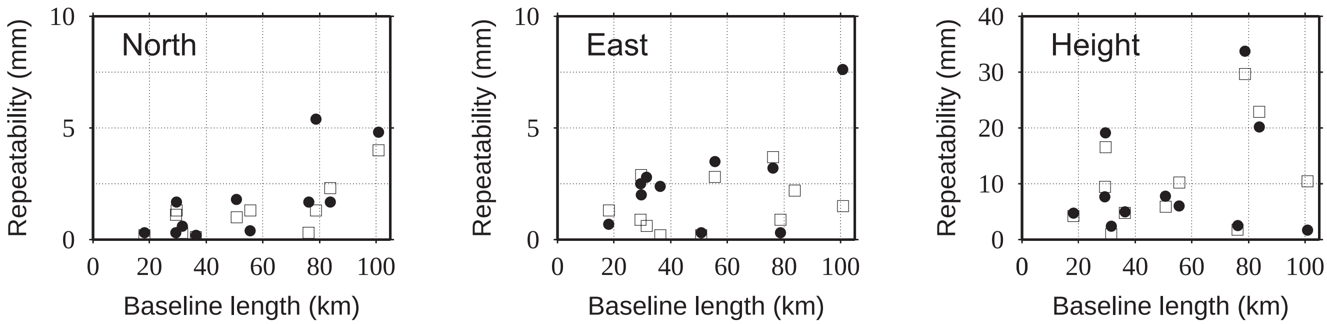

Figure 3: Station repeatabilities versus baseline length for the 1994 GPS solution using broadcast orbits (solid circles) and precise orbits from the International GPS Service for Geodynamics (open squares). Just the 11 stations used in the interpretation are displayed.

established in 1967 was now measured with GPS receivers for the first time, and a few new bench marks were established. Only four GPS stations are common to all three surveys.

We used three Trimble 4000 SST GPS receivers in the measurements. The station ISAK was used as a reference station, and one receiver was situated there during the whole survey. The measurement interval was 15 s, and the satellite elevation mask angle was 15°. Data from all visible satellites were collected, but their number varied from four to nine. About 16-22 hours data were collected for each station. The antenna was set up only once at each station. The measurements were conducted from July 18 to July 29 and from August 30 to September 17. Station occupation on a daily basis is given by *Jónsson et al.* [1995].

We analyzed the data using the Bernese GPS software version 3.5 [*Rothacher et al.,* 1993]. The coordinate solution is ambiguity fixed, and it was made in three steps; each step was executed for each day of the data set. First, the station coordinates were estimated using the ionospheric-free (L3) linear combination without fixing ambiguities. Second, ambiguities of the wide lane (L5) linear combination were resolved by keeping estimated coordinates from the first step fixed. Third, the final station coordinate solution was produced using the ionospheric-free linear combination by introducing the wide lane ambiguities from the second step. These three steps were completed twice, using two different types of orbital information: the broadcast orbit and the precise IGS orbit information. Repeatabilities for the 11 stations used in the interpretation of the GPS results are shown in Figure 3.

We used the Dynamic Adjustment Program (DYNAP) from the U.S. National Geodetic Survey [*Drew and Snay,* 1989] to compute a weighted network solution for all the data set and to produce baseline statistics, for both the broadcast and precise orbit solutions. Inputs for the program were coordinate and covariance files calculated for each observation day using the Bernese software. DYNAP was used to compute a weighted least squares network adjusted solution which includes full correlations in the weighting, giving final coordinates and coordinate uncertainty (Table 1).

Results of Electronic Distance Measurements

The Measurements

Distance measurements were conducted along the entire distance profile in 1967, 1973, 1977, and 1986, and a part of the profile was measured in 1970. Various models of geodimeters from the AGA cooperation in Sweden were used in these measurements (Table 2). The results of profile measurements for 1967-1986 have been reported in the work of *Decker et al.* [1971, 1976], and *Erlingsson and Einarsson* [1995]. In 1994, the profile was measured with GPS receivers for the first time.

Accuracy reported by the manufacturer for models AGA 6 and 8 is the same, with the root-mean-square error given as $\sigma = 5\,\mathrm{mm}+1$ ppm. Model 14A has higher root-mean-square error, or $\sigma = 5\,\mathrm{mm}+5$ ppm, but each measurement takes much shorter time giving higher number of observation and therefore better estimation of the mean and the standard deviation [*Erlingsson and Einarsson,* 1995].

Before different surveys along the profile were compared, we calculated a correction factor between the instruments used. The correction is calculated by comparing measurements on two calibration lines which are located in a tectonically stable area outside our study area. These lines are 3.0 and 5.2 km long, that is, within the range of most of the measured lines in the surveys.

The calculated correction does not contain a scale factor since the difference between measured length changes of the two calibration lines is insignificant. Corrections for all the profile surveys are given with respect to the 1967 results (Table 2). Uncertainties used for results of the distance measurements in this study are 1σ uncertainty, which fully include the uncertainties of the corrections (Table 2). Cumulative length changes along the profile are shown in Figure 4.

The western half of the profile was measured in 1970, just after the Hekla volcano erupted. Contraction was observed on the four westernmost profile segments in 1967-1970, but the next five showed extension. A total contraction of 88 ± 41 mm was observed between 1967 and 1973, and continuing contraction was detected until 1977.

Table 1: Various Information About GPS Surveys in the EVRZ in 1986, 1992, and 1994

	1986 Survey	1992 Survey	1994 Survey
Measurements			
Number of stations	51 (8 used)	41 (8 used)	42
Instruments	TI-4100	Trimble 4000 SST	Trimble 4000 SST
Analysis			
Software	Bernese version 3	Bernese version 3.3	Bernese version 3.5
Ephemeris used	broadcast	IGS/broadcast	IGS/broadcast
Reference system	WGS-72	ITRF-91/WGS-84	ITRF-92/WGS-84
Source of information	*Foulger et al.* [1993]	*Sigmundsson et al.* [1995]	this study
Estimated uncertainty, mm			
North-south	12	2.7 / 4.1	3.3 / 4.3
East-west	11	2.0 / 4.5	2.6 / 3.4
Vertical	23	11 / 12	7.8 / 10

IGS, International GPS Service for geodynamics; WGS, World Geodetic System; ITRF, IERS Terrestrial Reference Frame; IERS, International Earth Rotation Service.

A total contraction of 168 ± 44 mm was observed along the entire profile between 1967 and 1977.

The observed deformation pattern changed after 1977. An insignificant extension of 35 ± 65 mm is observed between 1977 and 1986. Extension continued after 1986 and a total extension of 138 ± 47 mm was observed between 1977 and 1994. The contraction observed in 1967-1977 and the extension observed in 1977-1994 together show no significant total change, -30 ± 39 mm, for the entire period 1967-1994.

One distinct feature can be seen in the results. Most of the movements (i.e., the contraction in 1967-1977 and the extension in 1977-1994) are taken up by the western part of the profile, when almost no significant movements are observed in the eastern part.

Table 2. Corrections for the Profile Surveys, Calculated From Measurements of Two Calibration Lines.

Year	Instrument	Correction, mm
1967	AGA model 6	0
1970	AGA model 8	-21 ± 5
1973	AGA model 8	-22 ± 4
1977	AGA model 8	-13 ± 5
1986	AGA model A14	-13 ± 6
1994	Trimble 4000 SST	-4 ± 4

Observed length changes along the profile are most probably due to horizontal changes but not due to normal faulting since graben-like structures in the vicinity of the profile are insignificant. Also, the profile segments are all tilted less than 3°, except one segment which is tilted 7°; therefore the effect from vertical changes is minor.

Profile Discussion

If $(85 \pm 15)\%$ of the total spreading in south Iceland is currently taken up by the EVRZ, as suggested by *Sigmundsson et al.* [1995], then about 450 mm total widening can be expected there in 27 years. A uniform widening of 450 mm in a direction of N104°E, occurring between the endpoints of the profile, would result in about 390 mm cumulative lengthening along it. This extension could easily be detected by the measurements along the profile during the years, and it is therefore clear that if this widening occurred during 1967-1994 then it was taken up out of the range of the profile. However, the estimate of *Sigmundsson et al.* [1995] was based on GPS results from 1986, 1989, and 1992. We observe 103 ± 62 mm extension along the whole profile between 1986 and 1994, which represents lengthening of about 116 ± 130 mm in the direction of N104°E, or an extensional rate of about 15 ± 16 mm/yr. The high uncertainty is caused by the projection of the profile results to a line with azimuth N104°E and the accumulated uncertainty when adding together changes of 23 profile segments. This rate is about 79% of the overall total average widening of 19 mm/yr, estimated by *DeMets et al.* [1994]. Our results are therefore consistent with those of *Sigmundsson et al.* [1995] for this period.

The contraction observed along the profile in 1967-1977, on the other hand, was not expected, considering that the profile crosses a divergent plate boundary. In an attempt to explain this phenomenon, we look critically at the observations again; are there any possibilities of unmodeled systematic errors between surveys, leading to tectonically unrealistic results? Since the western part of the profile shows significant deformation but the eastern part seems to be more or less stable (Figure 4), it indicates that unmodeled errors are not likely to be affecting the results. If we would explain the observed deformation along the western part of the profile as unmodeled systematic error, these errors should also cause significant changes at the eastern part of the profile (where little de-

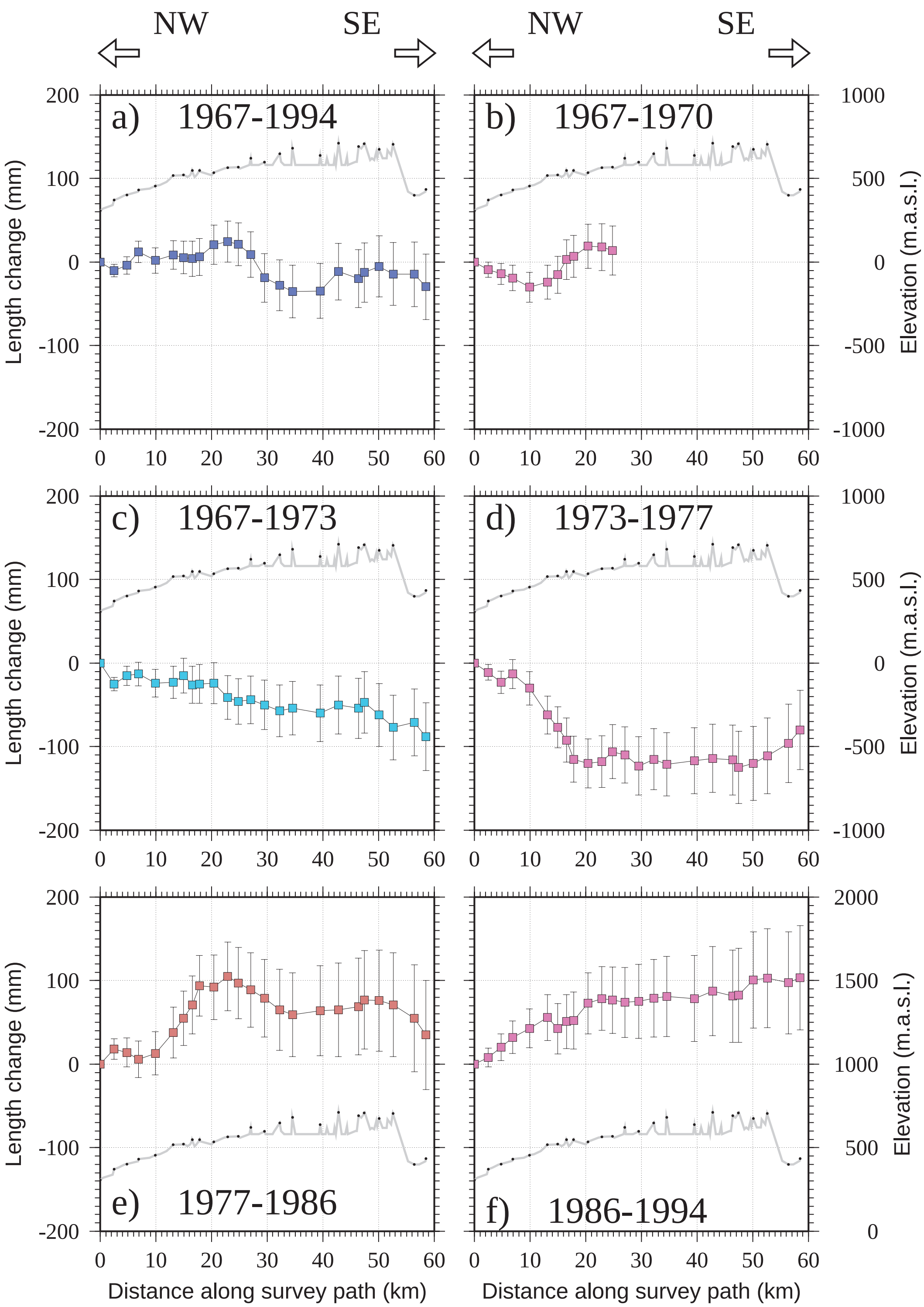

Figure 4: Cumulative length change along the distance profile relative to station 3350 (see Figure 2c) for different combinations of surveys. Error bars denote 1σ uncertainty. The topography along the profile is shown as a gray line.

formation is observed). Furthermore, the eastern part of the profile extends across much rougher topography than the western part, and it is therefore more likely to contain unmodeled errors (Figure 4). Also, the observed disturbances on the western part of the profile coincide with the tectonic and seismic activity in the area. Eruptions in Hekla occurred in 1970, in 1980-1981, and in 1991, and the Vatnafjöll earthquake ($M_w = 5.9$) occurred in 1987 (Figure 1b). No tectonic events and very little seismic activity have taken place near the eastern part of the profile, where small changes are observed.

The observed deformation along the profile during

1967-1977 is therefore most likely real, about 17 ± 4 mm/yr contraction, or a compressional strain rate of about 0.29 ± 0.08 μstrain/yr. Contraction was also observed across the Krafla fissure swarm in north Iceland in 1965-1971, prior to the 1975-1984 rifting episode [*Möller and Ritter,* 1980]. Up to about 0.5 ± 0.2 m contraction was observed across a 100 km wide network, or a compressional strain rate of about 0.8 ± 0.3 μstrain/yr.

Most of the contraction observed in 1967-1977 is taken up by the 10 westernmost segments of the profile (Figure 4). The contraction along this part of the profile is equivalent to a compressional strain rate of about 0.69 ± 0.12 μstrain/yr and requires further discussion. In order to try to explain this deformation, we look at likely effects from the Hekla eruptions on the profile points. Hekla's center is located at $63°59'31''$N and $19°40'02''$W, at a distance of about 22 km from the nearest point of the profile. As an example of the effect that could be caused by Hekla on the profile, we take best fit parameters from *Sigmundsson et al.* [1992a] of a Mogi point source model of the subsidence during the Hekla eruption 1991, estimated from results of GPS measurements around the volcano in 1989-1991. The predicted effect on a point at a distance of 22 km is about 18 mm movement toward the volcano. Relative movements between the profile points are very small in this example, leading to cumulative length change of only about -3 mm along the 10 most westerly segments of the profile but not 79 ± 38 mm as observed in 1986-1994.

The GPS measurements of *Sigmundsson et al.* [1992a] cover one period of deflation in Hekla. The magnitude of the deflation, following an eruption, is a function of the volume of material erupted and the depth to the point source. The estimated volume of the lava erupted in 1991 is 0.15 km^3 [*Gudmundsson et al.,* 1992], or similar to the volume estimates of lava erupted in 1970 and 1980-1981 [*Thórarinsson and Sigvaldason,* 1972a; *Grönvold et al.,* 1983]. If we assume that the point source is at the same location, similar effects would be expected from the former eruptions. The observed deformation along the western part of the profile therefore cannot be explained by a simple Mogi point source located beneath Hekla.

The epicenter of the Vatnafjöll earthquake ($M_w = 5.9$) in 1987 was at $63°54'36''$N and $19°46'48''$W [*Bjarnason and Einarsson*, 1991] at a distance of about 32 km from the nearest point on the profile. An earthquake of magnitude 5.9 produces little deformation at this distance [*Sigmundsson et al.,* 1995] and would cause insignificant relative movements between the profile points.

It is difficult to explain the observed deformation along the profile as a result of the tectonic events in the area. The observed deformation disturbances coincide, however, with the area of tectonic unrest. The conclusion is that even though the tectonic events may not easily explain the observations, the disturbances are probably caused by some common underlying process, leading to crustal deformation, eruptions, and earthquakes.

Displacements Determined by GPS

The 1986-1994 Displacements

The GPS data of 1986 and 1994 were processed using the Bernese software, versions 3 and 3.5, respectively. The software has gone through considerable development since version 3. However, most changes do not concern the modeling of the observables themselves. Therefore we believe that systematic errors due to software changes are small.

The coordinate solution from 1986 is in the World Geodetic System (WGS-72) [*Foulger et al.,* 1993], but it was transformed to the WGS-84 system. We used the broadcast orbit coordinate solution from 1994 to compare to the 1986 coordinates since it is also in the WGS-84 coordinate system. The average 1σ uncertainty of the horizontal displacements for 1986-1994 is estimated about 12 mm, and it is completely dominated by the 1986 position uncertainties.

During 1986-1994, displacements of six stations are consistent with a linear extension across the rift zone, but displacements of two stations (ISAK and station 3359) are inconsistent with this pattern (Figure 5). Station ISAK is close to the Hekla volcano, and it is well within the deformation field of the eruption of Hekla in 1991 [*Sigmundsson et al.,* 1992a]. On the other hand, the observed displacement of station 3359 may reflect an erratic movement of this point or is due to problems in processing of the 1986 data from this station.

All possible line-length changes between observed stations in 1986-1994 (except ISAK and 3359) were calculated, and a uniform strain field was fitted to them (Figure 6). Since the line-length changes are independent of rotation and translation of coordinate systems, the uncertainties in rotation and translation parameters in the WGS-72→WGS-84 transformation of the 1986 coordinates do not affect our results. In a uniform strain field, the strain along the azimuth θ is given by [*Sturkell et al.,* 1994]

$$\frac{dL}{L} = \frac{\varepsilon_1 + \varepsilon_2}{2} + \frac{\varepsilon_1 - \varepsilon_2}{2} \cos 2(\theta - \phi), \qquad (1)$$

where L is the line length, dL is the line-length change, ε_1 and ε_2 are principal strains, and ϕ is the azimuth of ε_1. We used a least squares analysis to solve for the three parameters, ε_1, ε_2, and ϕ, simultaneously. The average principal strain rates for 1986-1994 are

$$\dot{\varepsilon_1} = 0.12 \pm 0.01 \ \mu\text{strain/yr at N}135 \pm 5°\text{E}$$
$$\dot{\varepsilon_2} = -0.12 \pm 0.04 \ \mu\text{strain/yr at N}45 \pm 5°\text{E}.$$

The strain analysis indicates that the direction of maximum expansion is N$(135 \pm 5)°$E or perpendicular to the rift axis (Figure 6). The strain is equivalent to 85 ± 10 mm extension across the 90 km wide network during 8 years or 11 ± 1 mm/yr.

The best fitting uniform strain field indicates a compressional strain rate of 0.12 ± 0.04 μstrain/yr in direction of N$45 \pm 5°$E. However, relative displacements are not significant at the 95% confidence level in this direction. This strain rate is predominantly determined by the relative movement of the stations with respect to station JOKU,

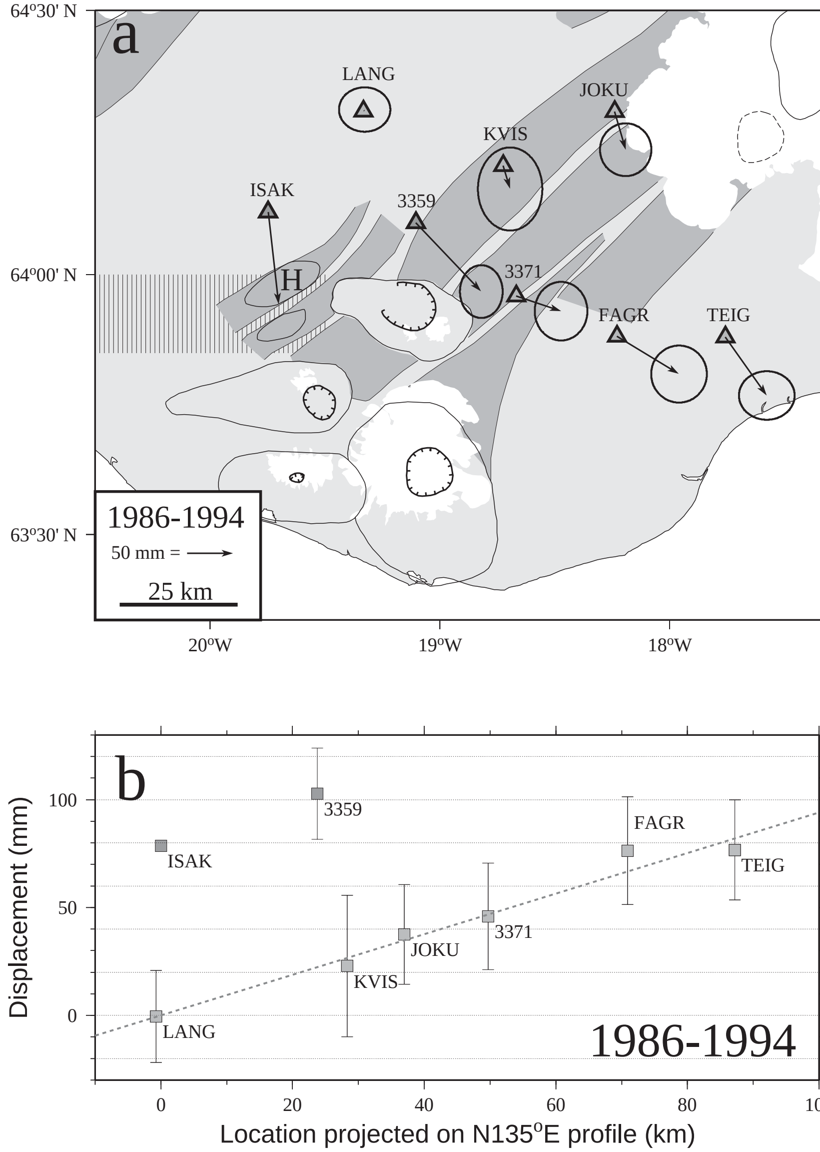

Figure 5: (a) The displacement field for 1986-1994 with 95% confidence ellipses relative to the reference station ISAK, after a rigid body translation of 10 mm in east and 102 mm in south has been applied, that is, the observed relative movement between station ISAK and LANG. H denotes Hekla. (b) Displacements in the direction of maximum extension, that is, N135°E. Error bars indicate 2σ uncertainty. The line indicates the best fitted strain; it has a slope of 0.94 ± 0.11 mm/km.

and the error margins would be higher if effects of correlation are taken into account when the best fitting strain field is found.

The displacement of the reference station ISAK, relative to the other station (LANG) west of the rift zone, is observed 102 ± 15 mm in the direction N174°E (Figure 5). Most of this displacement is presumably due to the deflation of Hekla, following the eruption in 1991. *Sigmundsson et al*. [1992a] measured the displacement of ISAK as 44 mm (N156°E) relative to a point at a distance$\geq$100 km during 1989-1991. Their best fit Mogi point source model of subsidence in Hekla predicts 49 mm (N169°E) displacement of ISAK during 1989-1991. The Vatnafjöll earthquake in 1987 ($M_w = 5.9$) may also explain part of the estimated displacement of ISAK, but it occurred at a distance of 23 km from ISAK.

No relative vertical movements were observed to be significant, except that all stations were uplifted relative to the reference station ISAK. This indicates a subsidence of that station, following the deflation of the Hekla volcano when it erupted in 1991. The average uplift of the stations in the network relative to ISAK is 45 ± 9 mm, and it can be used as an estimate of the subsidence of that station.

The 1992-1994 Displacements

The GPS data of 1992 and 1994 were processed using the Bernese software, versions 3.3 and 3.5, respectively. The software went through significant modifications between versions 3.3 and 3.5. However, the most important changes were improvements of the ambiguity resolution algorithms, which give more reliable results. In the 1992 coordinate solution, 79% of the ambiguities were resolved, and the horizontal position uncertainties were estimated to be 4 mm by studying the scatter in the solution between independent sessions. In the 1994 coordinate solution, 87% of the ambiguities were resolved.

The best coordinate solution from 1992 is in the IERS Terrestrial Reference Frame (ITRF-91). Our solution obtained from the IGS precise orbits is in the ITRF-92 system. The difference between these two systems is small, less than 20 mm in translation, with no rotation and insignificant scale factor for this network [*Boucher et al.,* 1993]. Therefore the solutions from 1992 and 1994 can be compared directly. The average 1σ uncertainty of the horizontal displacements for 1992-1994 is about 5 mm.

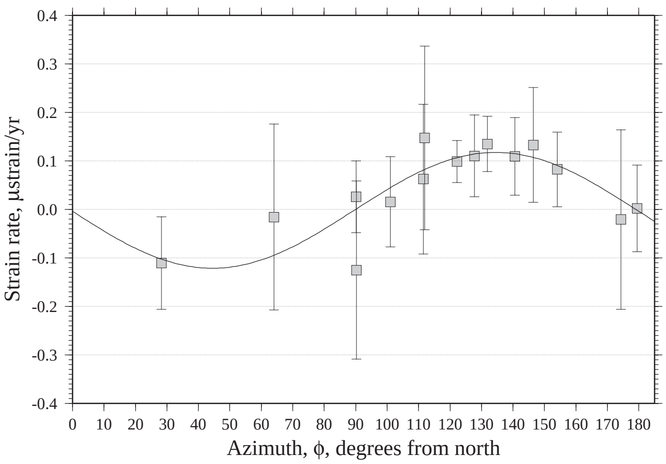

Figure 6. Strain rates for lines between stations in the period 1986-1994 as a function of the azimuth of the lines. Error bars denote 2σ uncertainty. The sinusoidal line indicates the best fitting uniform strain field.

When the reference station ISAK is held fixed, the six points to the east of it show movements to the east or southeast (Figure 7a). Two-dimensional strain analysis, similar to those used for the 1986-1994 results, is not suitable for the 1992-1994 results since the stations are located, more or less, along a NW-SE line. The best fit line of the N135°E displacements in Figure 7b has the slope 0.24 ± 0.05 mm/km, equivalent to 26 ± 6 mm extension across the 110 km wide network between 1992 and 1994, or 13 ± 3 mm/yr. The observed strain rate across the network for 1992-1994 in the direction N135°E is 0.12 ± 0.03 µstrain/yr, or equivalent to the strain rate, 0.12 ± 0.01 µstrain/yr, observed for 1986-1994 in the same direction. No significant relative movements are observed in the direction N45°E at 95% confidence level for 1992-1994. The reference point ISAK was included in the calculations above. It seems that the effect from Hekla, observed in 1986-1994, took place before 1992. Hardly any significant vertical displacements are observed in 1992-1994, and they seem not to follow a systematic pattern.

GPS and the Distance Profile

Both the GPS measurements and the distance measurements of the profile cover the period from 1986 to 1994. No GPS measurements were conducted before 1986. The GPS results and the profile results for 1986-1994 are plotted together in Figure 8. The GPS displacements are plotted relative to the reference station ISAK in the direction of maximum widening, N135°E. The cumulative changes of the profile are calculated as $\sum \Delta d_i / \cos(\theta_i - 135)$, where Δd_i is observed length change of profile segment i and θ_i is the orientation of the segment. The cumulative length change in the direction of N135°E is displayed relative to station 3371, where the profile results intersect the GPS results.

The profile results fit well with the GPS results along the eastern part of the profile (Figure 8). The modified cumulative length change along the western part of the profile indicates more extension than observed with GPS. However, this extension is compatible with the GPS results except for the profile segment between stations 3358 and 3359. The observed lengthening of the 3358-3359 segment is 21 ± 14 mm, an extension of 43 ± 29 mm in direction N135°E is required to explain the lengthening of this segment which is aligned at 61° from N135°E. The 1986-1994 GPS results revealed an anomalous displacement of station 3359. If we explain it as an erratic displacement, it is compatible to the profile results for the segment 3358-3359 but not for the segments 3359-3371 (Figure 8). Therefore the anomalous displacement may be due to processing problems. In summary, by ignoring station 3359, the profile results and the GPS results are in agreement with each other.

A strain analysis using results from both the profile and the GPS measurements was performed for the period 1986-1994. The profile results do not improve the strain analysis. The reason is that the GPS baselines are about 10 times longer and better estimated than the profile lines, and therefore they play the leading role in the determination of the strain field.

Modeling the Observed Crustal Deformation

We now attempt to model the observed deformation as postrifting effects of the most recent rifting events in the EVRZ. The following five different models have been applied to explain observed postrifting deformation following the rifting episode in Krafla, north Iceland, in 1975-1984: (1) an emplacement of an infinitely long dike into an elastic layer, underlain by a Newtonian viscous layer [*Foulger et al.,* 1992], (2) the same model except for a dike with finite length [*Heki et al.,* 1993], (3) a continuous dike intrusion at depth into an elastic half-space [*Hofton,* 1995; *Hofton and Foulger,* 1996], (4) a finite length dike intrusion in an elastic layer, overlying a half-space of Maxwell viscoelastic material [*Hofton,* 1995; *Hofton and Foulger,* 1996], and (5) a finite length dike intrusion in an elastic layer on a spherically viscoelastic Earth model [*Pollitz and Sacks,* 1996].

In order to explain the observed deformation in the

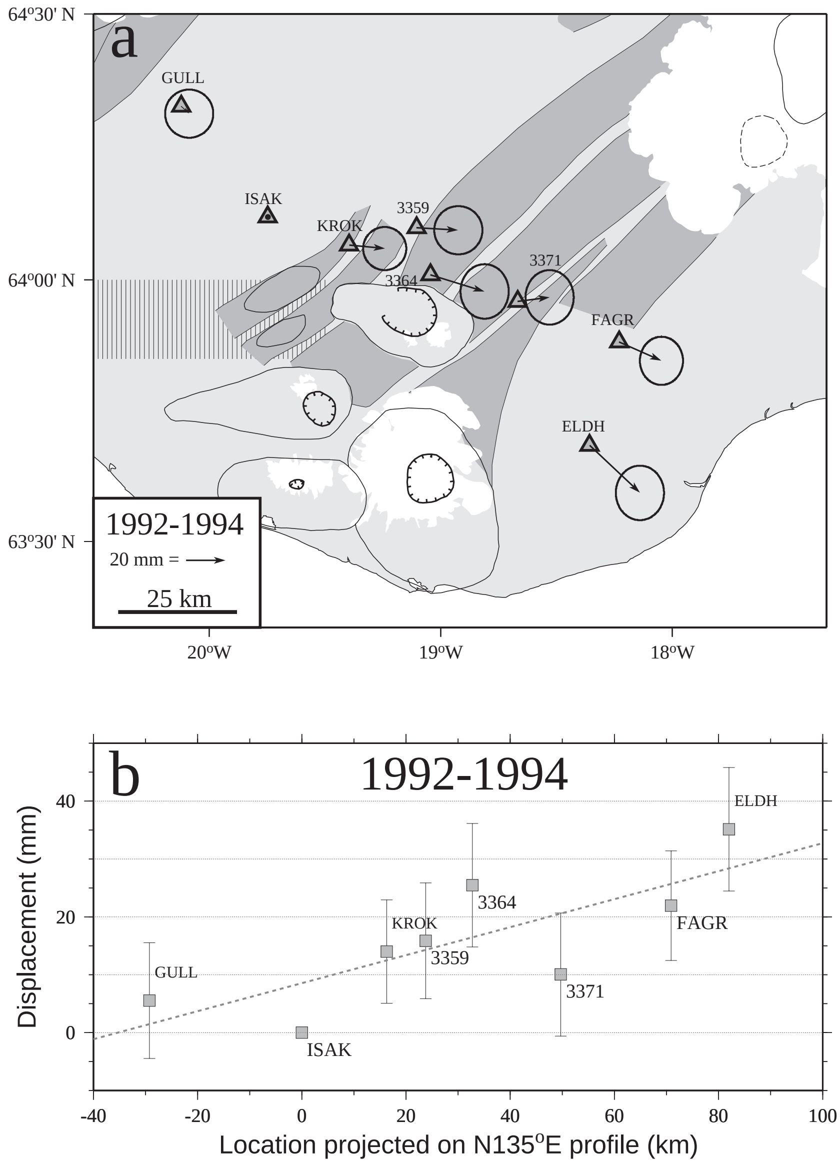

Figure 7: (a) The displacement field for 1992-1994 with 95% confidence ellipses relative to station ISAK. (b) Displacements in the N135°E. Error bars indicate 2σ uncertainty. The line indicates the best fitted strain; it has the slope 0.24 ± 0.05 mm/km.

EVRZ, we apply the first one of these postrifting geodynamic models. The most recent rifting episodes in the area are modeled, and their predicted contribution to the present deformation field is computed. In our view, the data at hand do not warrant more sophisticated modeling.

Following *Foulger et al.* [1992], we assume an elastic layer with thickness h overlying a Newtonian viscous layer with thickness b, which is underlain by a rigid half-space (Figure 9). An infinitely long dike is intruded through the entire elastic layer at time $t_0 = 0$. The problem is one-dimensional, with horizontal displacements, $u(x,t)$, depending on time and the distance perpendicular from the dike.

By assuming that the velocity at the base of the viscous layer is zero and the viscous flow can be approximated by linear Couette flow and by assuming plane stress and plain strain conditions, it can be shown that the equation of motion is equal to the diffusion equation [*Elsasser,* 1969; *Foulger et al.,* 1992; *Heki et al.,* 1993; *Jónsson,* 1996]:

$$\frac{\partial u}{\partial t} = \kappa \frac{\partial^2 u}{\partial x^2} \tag{2}$$

with a diffusivity κ:

$$\kappa = \frac{bhM}{\eta}, \tag{3}$$

where h and b are the elastic and viscous layer thicknesses, η is the viscosity, and $M = 4\mu(\lambda+\mu)/(\lambda+2\mu)$, where λ and μ are the Lamé elastic moduli of the uppermost layer. Assuming dike intrusion of thickness $2U_0$, an appropriate solution of equation (2) is [*Carslaw and Jaeger,* 1959]:

$$u(x,t) = U_0 \operatorname{erfc} \frac{x}{2\sqrt{\kappa t}} \tag{4}$$

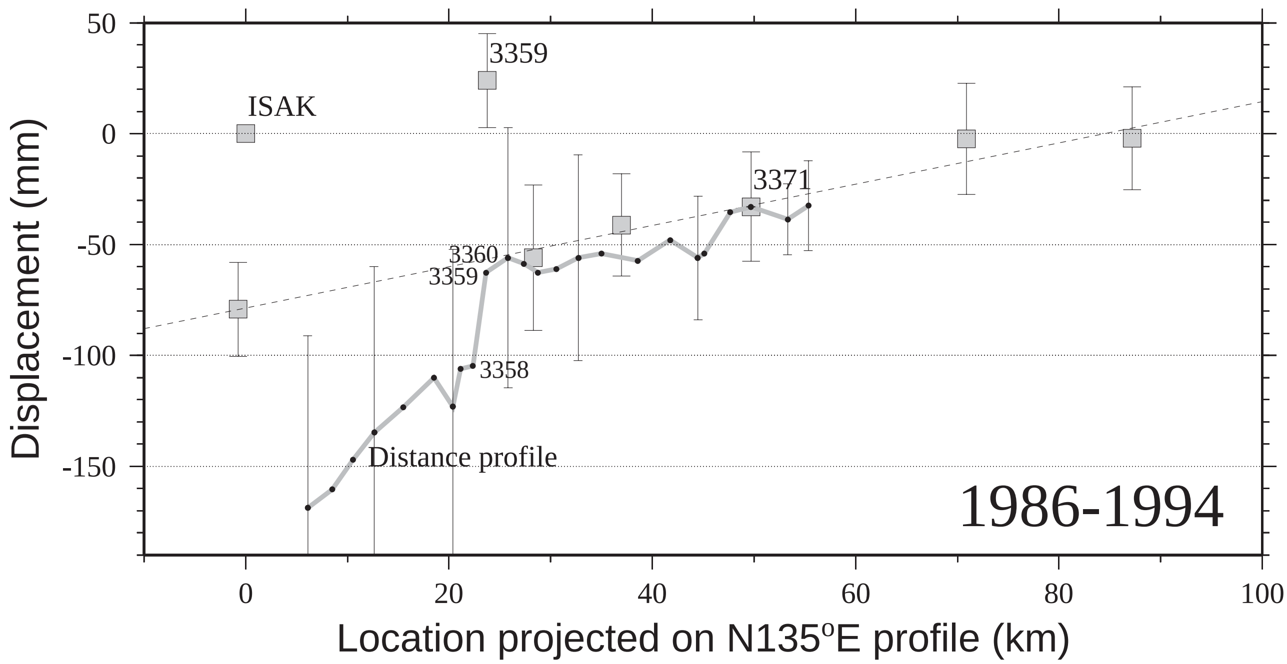

Figure 8: The 1986-1994 GPS displacements in the direction of maximum extension (N135°E) relative to station ISAK. Error bars indicate 2σ uncertainty. The results of the profile measurements are shown with solid gray line relative to station 3371, where they intersect the GPS results. Representative uncertainties (1σ) are displayed for a few profile points. The straight line indicates the best fitted uniform strain 0.94 ± 0.11 μstrain. The results of the electronic distance measurements are compatible with the GPS results if one of the profile segments (3358-3359) is ignored.

where erfc is the complementary error function. The corresponding velocity is

$$\frac{\partial u}{\partial t} = \frac{U_0}{t\sqrt{\pi}} \frac{x}{2\sqrt{\kappa t}} e^{-x^2/4\kappa t}. \tag{5}$$

Heki et al. [1993] point out that the current displacement, since the rifting began, may be written as the sum of the contribution from the latest episode, $u(x,t)$, and from a large number of past episodes, which they call "background" movement:

$$U(x,t) = u(x,t) + u_{background} = u(x,t) + \sum_{n=1}^{\infty} u(x, t+nT) \tag{6}$$

where T is the recurrence time interval of the rifting episodes.

By using recurrence time of about 100 years and dike halfwidth of $U_0 = 1$ m, we get time averaged spreading rate of 20 mm/yr. The background movement is the continuous part of the movements. It is zero at the boundary, but it is the same as the relative plate velocity in the far field, where no episodic movements occur.

Estimating the Rifting Episodes

The average overall spreading rate in south Iceland is estimated 19 mm/yr [*DeMets et al.,* 1994]. We assume that the most part of this widening has occurred in the EVRZ during the last few hundred years, as suggested by *Sigmundsson et al.* [1995], but much less in the parallel WVZ. Considering this, we try to estimate the magnitude of historical rifting episodes in the area. Major rifting episodes occurred in the area in 871 ± 2 [*Grönvold et al.,* 1995], circa 934, circa 1480, 1783-1784, and a smaller one occurred in 1862-1864 (Table 3 and Figure 10). We estimate the dike thicknesses due to these episodes as the product of time interval since the last rifting episode multiplied by the spreading rate.

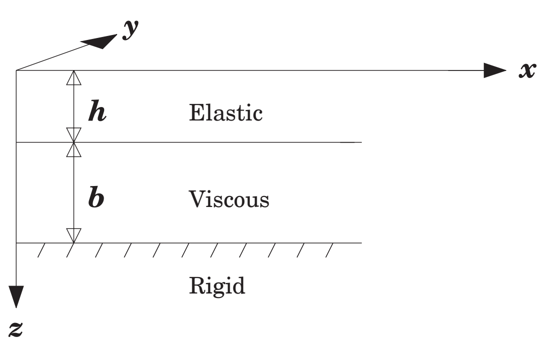

Figure 9. Schematic diagram of the elastic-viscous model. After *Foulger et al.* [1992], with permission from Nature, copyright 1992 Macmillan Magazines Ltd.

The Vatnaöldur and Eldgjá episodes around 900 A.D. occupied the whole rift zone, and it may be argued that they relieved the tectonic stress along the plate boundary. After tectonic rest of about 550 years, from circa 934 until circa 1480, we consider conditions in the zone ripe for a dike intrusion with thickness 550 years × 19 mm/yr or

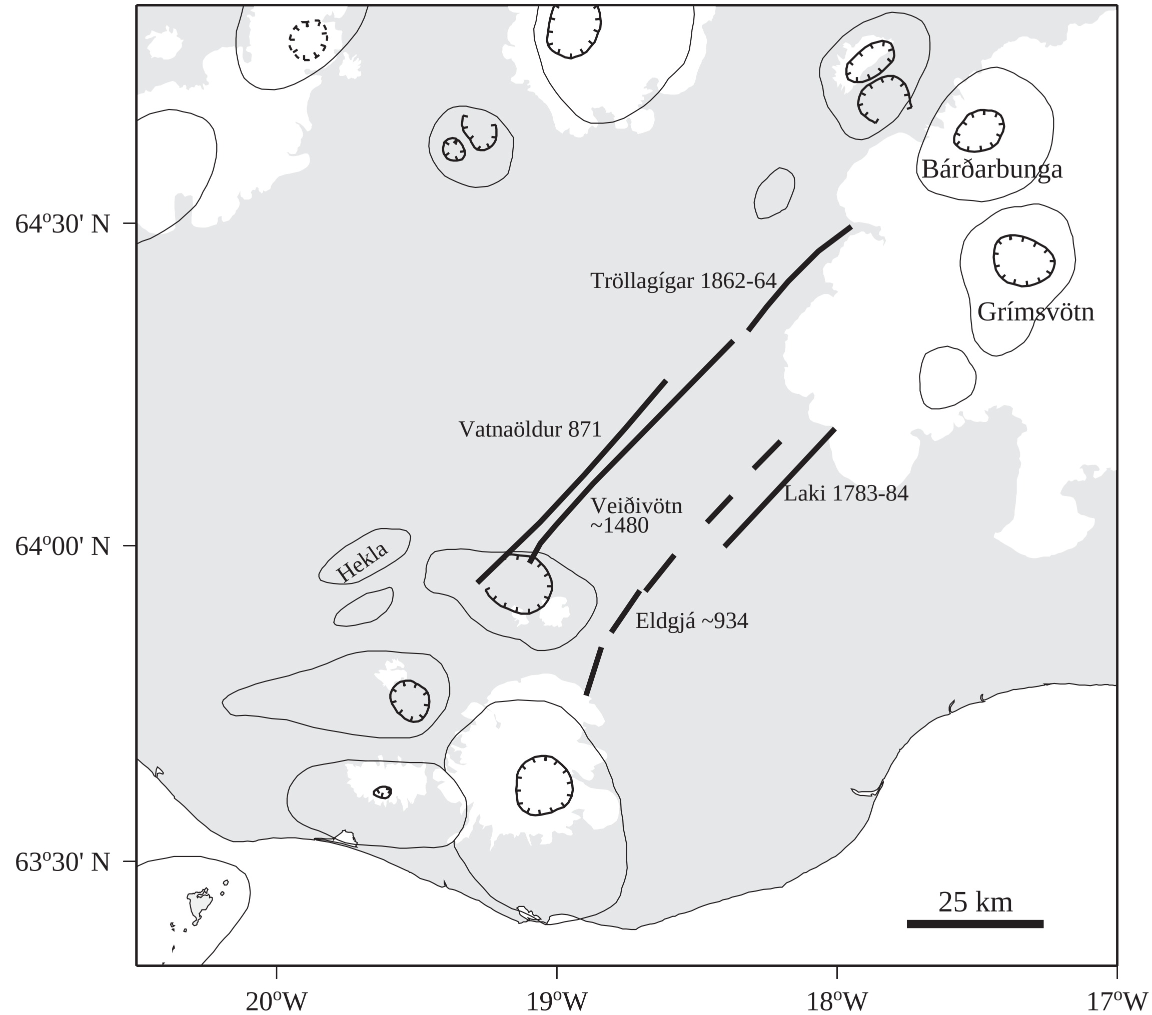

Figure 10: Major historical rifting episodes in the EVRZ. The solid lines indicate approximately the eruptive fissures, but some of them were discontinuous.

about 10 m. The Veidivötn eruption occurred in circa 1480 on a fissure at least 40 km long [*Larsen,* 1984]. The corresponding dike was longer, probably extending from the Bárdarbunga central volcano and along the entire EVRZ. We suggest therefore that the stress conditions in the rift zone after this episode were close to the initial ones.

Table 3. Major Rifting Episodes in the EVRZ During the Last 1100 Years, and a Rough Estimate of Thickness and Length of the Corresponding Intrusion.

Rifting Episode	Year	Dike Thickness, m	Dike Length, km
Vatnaöldur	871 ± 2		115
Eldgjá	~ 934		75
Veidivötn	~ 1480	10	105
Laki	1783-1784	4.5	70
Tröllagígar	1862-1864	1.5	45

The only evidence of rifting in the WVZ during the last 1000 years is subsidence and rifting in the Thingvellir graben in 1789. The subsidence is estimated as 1.0-2.6 m [*Sæmundsson,* 1992], and the corresponding dilatation of the graben was probably of similar magnitude. However, the Thingvellir graben dies out toward the northeast, and the rifting of 1789 probably did not take place along the entire WVZ. Therefore we estimate the rifting of the zone to be about 1 m. Together with the Laki rifting episode that occurred in 1783-1784 [*Thórdarson and Self,* 1993], the total rifting is estimated about 300 years $\times$ 19 mm/yr or about 5.5 m. The 4.5 m thick Laki dike is here considered to have extended from the Grímsvötn caldera in Vatnajökull and along most of the eastern rift zone.

The latest rifting episode, the Tröllagígar eruption in 1862-1864 [*Thórarinsson and Sigvaldason,* 1972b], occurred about 80 years after the Laki eruption. We estimate the corresponding dike thickness to be 1.5 m for this episode. We suggest that the dike extended from the Bárdarbunga system to the southwest, along half of the rift zone at least. By using this method, the present condition in the EVRZ would allow dike thickness exceeding

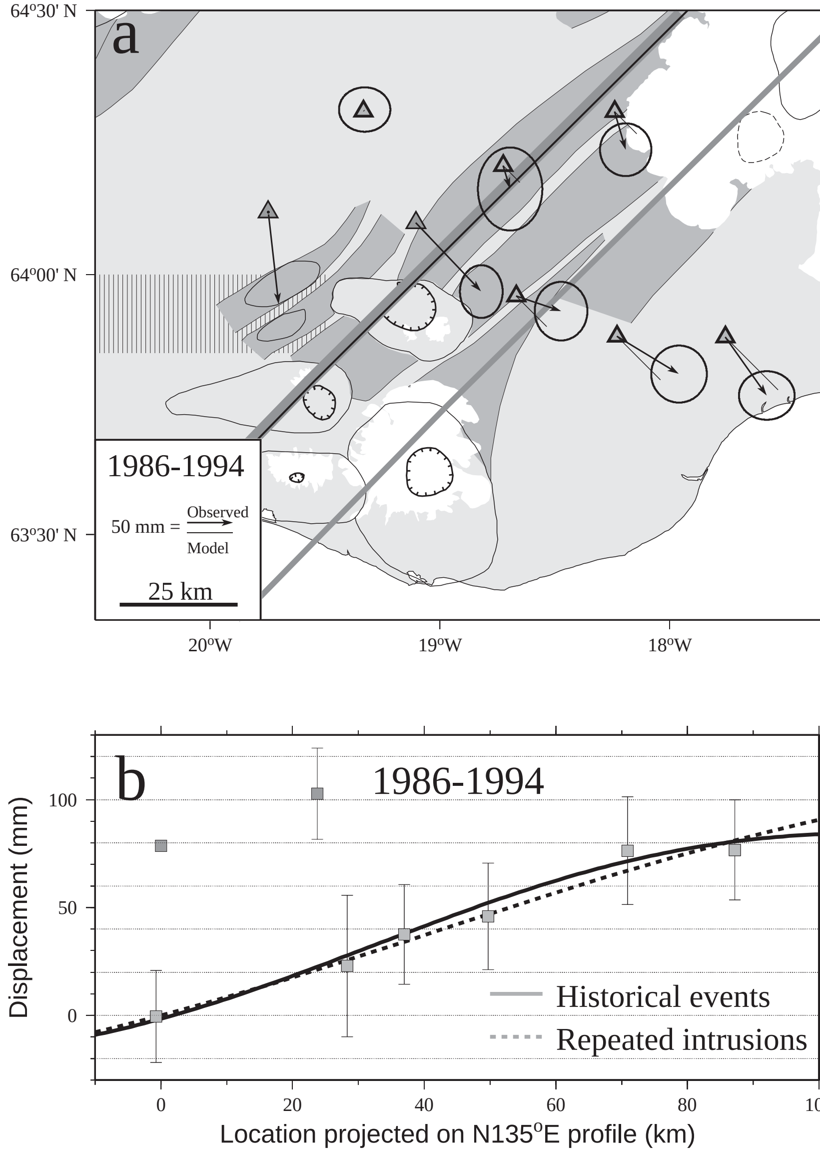

Figure 11: (a) The background model ($\kappa = 0.9$ m^2/s) and the observed displacement field for 1986-1994 with 95% confidence ellipses. Thick lines indicate locations of the dikes used in the modeling. (b) Displacements in southeast direction. The solid line shows the predicted contribution from the last three rifting episodes using a stress diffusivity of $\kappa = 0.3$ m^2/s. The dashed line shows background movement of repeated events with a recurrence time of 100 years and a stress diffusivity $\kappa = 0.9$ m^2/s.

2 m since about 130 years have passed from the latest rifting episode.

Fit of the Elastic-Viscous Model

Two different approaches were tried in order to see if the elastic-viscous model may simulate the observed deformation in the EVRZ. First, the effects from the rifting episodes in circa 1480, 1783, and 1862 were calculated using dike thicknesses in Table 3. Second, the background movement was calculated using recurrence time of 100 years and dike thickness of 1.9 m.

For the 1986-1994 GPS results, the best fit diffusivities are 0.9 m^2/s for the background model and 0.3 m^2/s for the model of the three episodes (Figure 11). The diffusivity will increase, in the latter case, if rifting episodes prior to circa 1480 are taken into account. For example, the Vatnaöldur and Eldgjá episodes were in many ways similar to the Veidivötn and Laki episodes, respectively. By assuming 10 m and 4.5 m thick dikes were intruded in 871 and 934 and adding the result to the three dikes model, we obtain a best fit diffusivity of 0.5 m^2/s for our 1986-1994 results. For the 1992-1994 GPS results, the best fit diffusivities are 0.8 m^2/s for the background model and 0.4 m^2/s for the model of the three episodes.

By using this one-dimensional model for north Iceland to explain postrifting crustal movements in 1987-1990, *Foulger et al.* [1992] found a diffusivity of 1.1 m^2/s. On the other hand, two-dimensional modeling by *Heki et al.* [1993] on the same observations gave a higher diffusivity, or $\kappa = 10$ m^2/s.

From equation (3), one can see that the diffusivity is equal to the ratio $(bhM)/\eta$. For north Iceland, *Foulger et al.* [1992] took $\lambda = \mu = 0.28 \times 10^{11}$ Pa, $h = 8 - 30$ km as the elastic layer thickness and the viscous layer thickness as $b = 5 - 10$ km. With these values and $\kappa = 0.3 - 0.9$ m^2/s, the calculated viscosity is $\eta = 0.3 - 7.5 \times 10^{19}$ Pa s. This result is compatible with viscosity values estimated from glacio-isostatic movements [*Sigmundsson,* 1990, 1991; *Sigmundsson and Einarsson,* 1992]. Even though the one-dimensional model fits the 1986-1994 measurement results well, it is not compatible with the results of the distance measurements for 1967-1977.

Discussion

Results of GPS and Electronic Distance Measurements

If the present uniform extension observed with GPS for 1986-1994 has a linear continuation to the southeast and northwest, then the total average spreading is accommodated in a zone less than 200 km wide. Even though the spreading in south Iceland may currently be equal to the total average spreading, as observed and suggested by *Sigmundsson et al.* [1995], our question is; Can we extrapolate the observed uniform and stable widening in 1986-1994 to a longer time period? According to the elastic-viscous model, we consider the answer to this question to be "yes". The answer is "no" if we consider the distance profile measurements prior to 1986, assuming that these results represent the regional deformation in the EVRZ, as they do 1986-1994. We know that movements are episodic at divergent plate boundaries, as clearly observed in north Iceland during and following the Krafla rifting episode [e.g., *Wendt et al.,* 1985; *Foulger et al.,* 1992]. However, episodic movements in the EVRZ, where no major rifting episode has occurred in the last 130 years, seem somewhat surprising.

What can cause the temporal fluctuations observed in the deformation field? Possible explanations for compressional movements along a line crossing a divergent plate boundary are few. One explanation would be a pressure drop in a magma reservoir near the line, but a Mogi point source model of the Hekla volcano gave insufficient movements along the distance profile. Another explanation could be that the line is close to an end of a dike intrusion and perpendicular to its strike. We have no seismological evidence for such dike intrusions associated with Hekla in the vicinity of the profile. Modeling such intrusions was therefore not pursued. The third explanation could be aseismic movements or pressure changes of large bodies below the crust, resulting in large-scale fluctuations. An upwelling mantle plume centered below Iceland and movements of its material along the spreading ridge, to the southwest and north, have been proposed [e.g., *Vogt,* 1974].

By eliminating the first and second explanation above, we are left with the third which is very general. The profile measurements show contraction in 1973-1977 and extension in 1977-1986, so something changed between 1973 and 1986. A period of tectonic unrest occurred in Iceland during this period. The Krafla rifting episode began in 1975, a sequence of earthquakes of magnitude $M \geq 5$ started in Bárdarbunga central volcano in 1974, Hekla erupted 1980 and 1981, and 1976-1977 was a period of unusually high seismic activity in the Katla volcano. Also, earthquake sequences were frequent in south and west Iceland, a magnitude 6.5 (M_s) earthquake occurred near the north coast, and the Grímsvötn volcano erupted in 1983. Perhaps these phenomena, the observed fluctuations and the tectonic unrest, represent a pulse in the mantle plume activity beneath Iceland.

Modeling of the Deformation Field

The elastic-viscous model is highly idealized and assumes many simplifications. The most important ones are the Newtonian viscous material, its linear flow, and the infinite dike length assumed. However, a finite dike length would probably not have changed the elastic-viscous modeling drastically. Historical dike intrusions at Veidivötn circa 1480 and Laki 1783-1784 extended through most of the measured network and far to the northeast. Their predicted contribution to the present deformation field in the measured network is probably similar in the one- and two-dimensional cases. On the other hand, the Tröllahraun rifting episode in 1862-1864 would give different pattern to the deformation since the associated dike is assumed to have extended along just half of the EVRZ. The two-dimensional elastic-viscous model of *Heki et al.* [1993] for the Krafla episode in north Iceland predicts little effect on points in the EVRZ. This model of Krafla predicts no displacements for 1987-1990 at a distance of 120 km from the end of the dikes, in the direction of the Krafla dikes [*Heki et al.,* 1993, Figure 6]. The network in the EVRZ is at a distance of about 200 km from the Krafla caldera.

Assuming Newtonian viscous layer in the modeling is a more important simplification, it subdues the immediate response of diking and overestimates the postdiking displacements [*Heki et al.,* 1993]. Hence the present contribution from historical rifting episodes in the EVRZ, calculated by using the elastic-viscous model, is probably overestimated. Thus more realistic models of the Earth may reveal that postdiking deformation from historical rifting episodes is currently too small to explain the uniform extension observed for 1986-1994.

We suggest that the contractional displacements observed across the EVRZ during 1967-1977 are due to a source different from postdiking deformation from historical dike intrusions in the rift zone, as previously discussed.

Conclusions

1. The GPS results indicate uniform extension within a 100 km wide network across the EVRZ of 0.12 ± 0.01 μstrain/yr during 1986-1994 and of 0.12 ± 0.03 μstrain/yr during 1992-1994.

2. Local deformation is observed in the vicinity of the Hekla volcano because of its subsidence during the eruption in 1991. This deformation took place before the 1992 survey.

3. The results of the distance profile measurements 1986-1994 are compatible with the GPS results if one of the profile segments is excluded (3358-3359). This indicates that the profile results may reflect the regional strain field in the EVRZ, also prior to 1986.

4. The distance profile measurements indicate contraction along the profile during 1967-1977 and extension during 1977-1994. The observed irregularities along the distance profile coincide with the area of tectonic unrest in the rift zone. We conclude that the disturbances are probably caused by some common underlying process leading to crustal deformation, eruptions, and earthquakes.

5. The measurement results from 1986-1994 can be simulated by a simple model of infinitely long dike intrusions into an elastic layer overlying a viscous layer.

Acknowledgments. The work was funded by the Icelandic Research Fund for Graduate Students, the Icelandic Science Fund, and the Research Fund of the University of Iceland. Karl Pálsson, Halldór Ólafsson, and Thráinn Fridriksson participated in the measurements, and the National Power Company provided logistic support. Thanks are due to Gillian R. Foulger for useful discussions and Michelle A. Hofton for providing programs and for discussions. We thank the Department of Geological Sciences, University of Durham (England), and G. R. Foulger for providing accommodation and equipment for part of the project. GMT programs were used to produce graphics [*Wessel and Smith,* 1995]. Thoughtful reviews by R. W. King, K. L. Feigl, and Z. Shen improved the paper.

References

Beutler, G., E. Brockmann, W. Gurtner, U. Hugentobler, L. Mervart, M. Rothacher, and A. Verdun, Extended orbit modeling techniques at the CODE processing center of the international GPS service for geodynamics (IGS): Theory and initial results, *Manuscr. geod., 19*, 367-386, 1994.

Bjarnason, I. Th., and P. Einarsson, Source mechanism of the 1987 Vatnafjöll earthquake in south Iceland, *J. Geophys. Res., 96*, 4313-4324, 1991.

Björnsson, H., and P. Einarsson, Volcanoes beneath Vatnajökull, Iceland: Evidence from radio echo-sounding, earthquakes and jökulhlaups, *Jökull, 40*, 147-168, 1990.

Boucher, C., Z. Altamimi, and L. Duhem, ITRF 92 and its associated velocity field, *IERS Tech. Note 15*, 142 pp., Int. Earth Rotational Serv., Paris, 1993.

Carslaw, H. S., and J. C. Jaeger, *Conduction of Heat in Solids,* 550 pp., Oxford Univ. Press, New York, 1959.

Decker, R. W., P. Einarsson, and P. A. Mohr, Rifting in Iceland: New geodetic data, *Science, 173*, 530-533, 1971.

Decker, R. W., P. Einarsson, and R. Plumb, Rifting in Iceland: Measuring horizontal movements, *Greinar, 5,* 61-71, Vísindafélag Ísl., Reykjavík, Iceland, 1976.

DeMets, C., R. G. Gordon, D. F. Argus, and S. Stein, Effect of recent revisions to the magnetic reversal time scale on estimates of current plate motions, *Geophys. Res. Lett., 21,* 2191-2194, 1994.

Drew, A. R., and R. A. Snay, DYNAP: Software for estimating crustal deformation from geodetic data, *Tectonophysics, 162,* 331-343, 1989.

Einarsson, P., Earthquakes and present-day tectonism in Iceland, *Tectonophysics, 189*, 261-279, 1991.

Einarsson, P., and J. Eiríksson, Earthquake fractures in the districts Land and Rangárvellir in the SISZ, *Jökull, 32*, 113-120, 1982.

Einarsson, P., and K. Sæmundsson, Earthquake epicenters 1982-1985 and volcanic systems in Iceland (map), in: *Í Hlutarins Edli: Festschrift for Thorbjörn Sigurgeirsson,* edited by Th. Sigfússon, Menningarsjódur, Reykjavík, 1987.

Elsasser, W. M., Convection and stress propagation in the upper mantle, in *The Application of Modern Physics to the Earth and Planetary Interiors,* edited by S. K. Runcorn, pp. 223-246, Wiley-Interscience, New York, 1969.

Erlingsson, S., and P. Einarsson, Distance measurements across the rift zones in southern Iceland, 1967-1986, *Rep. RH-10-95*, 34 pp., Sci. Inst., Univ. of Iceland, Reykjavík, 1995.

Foulger, G. R., C.-H. Jahn, G. Seeber, P. Einarsson, B. R. Julian, and K. Heki, Post rifting stress relaxation at the divergent plate boundary in northeast Iceland, *Nature, 358*, 488-490, 1992.

Foulger, G. R., et al., The Iceland 1986 GPS geodetic survey: Tectonic goals and data processing results, *Bull. Géod., 67*, 148-172, 1993.

Grönvold, K., G. Larsen, P. Einarsson, S. Thórarinsson, and K. Sæmundsson, The Hekla eruption 1980-1981, *Bull. Volcanol., 46*, 349-363, 1983.

Grönvold, K., N. Óskarsson, S. J. Johnsen, H. B. Clausen, C. U. Hammer, G. Bond, and E. Bard, Ash layers from Iceland in the Greenland GRIP ice core correlated with oceanic and land sediments, *Earth Planet. Sci. Lett., 135,* 149-155, 1995.

Gudmundsson, A., Tectonics of the Thingvellir fissure swarm, SW Iceland, *J. Struct. Geol., 9*, 61-69, 1987.

Gudmundsson, A., et al., The 1991 eruption of Hekla, Iceland, *Bull. Volcanol., 54*, 238-246, 1992.

Heki, K., G. R. Foulger, B. R. Julian, and C.-H. Jahn, Plate dynamics near divergent boundaries: Geophysical implications of postrifting crustal deformation in NE Iceland, *J. Geophys. Res., 98*, 14,279-14,297, 1993.

Hofton, M. A., Anelastic deformation in Iceland studied using GPS, Ph.D. thesis, 258 pp., Univ. of Durham, England, 1995.

Hofton, M. A., and G. R. Foulger, Postrifting anelastic deformation around the spreading plate boundary, north Iceland, 1. Modeling of the 1987-1992 deformation field using a viscoelastic Earth structure, *J. Geophys. Res., 101*, 25,403-25,421, 1996.

Jakobsson, S. P., Chemistry and distribution pattern of recent basaltic rocks in Iceland, *Lithos, 5*, 365-386, Durham, 1972.

Jakobsson, S. P., Petrology of recent basalts of the Eastern Volcanic Zone, *Acta Nat. Isl., 26*, 103 pp., 1979.

Jónsson, S., *Crustal deformation across a divergent plate boundary, the Eastern Volcanic Rift Zone, south Iceland, 1967-1994, using GPS and EDM,* M.Sc. thesis, 165 pp., Univ. of Iceland, Reykjavík, 1996.

Jónsson, S., P. Einarsson, F. Sigmundsson, K. Pálsson, and H. Ólafsson, GPS experiments in the Eastern Volcanic Zone, south Iceland, in 1994, *Rep. RH-11-95*, 54 pp., Sci. Inst., Univ. of Iceland, Reykjavík, 1995.

Larsen, G., Recent volcanic history of the Veidivötn fissure swarm, Southern Iceland-An approach to volcanic risk assessment, *J. Volcanol. Geotherm. Res., 22*, 33-58, 1984.

Möller, D., and B. Ritter, Geodetic measurements and horizontal crustal movements in the rift zone of NE-Iceland, *J. Geophys., , 47*, 110-119, 1980.

Pollitz, F. F., and I. S. Sacks, Viscosity structure beneath northeast Iceland, *J. Geophys. Res., 101*, 17,771-17,793, 1996.

Rothacher, M., G. Beutler, W. Gurtner, E. Brockmann, and L. Mervart, Documentation for Bernese GPS software version 3.4, Univ. of Bern, Switzerland, 1993.

Sæmundsson, K., Fissure swarms and central volcanoes of the neovolcanic zones of Iceland, *Geol. J., Spec. Issue, 10*, 415-432, 1978.

Sæmundsson, K., Outline of the geology of Iceland, *Jökull, 29*, 7-28, 1979.

Sæmundsson, K., Geology of the Thingvallavatn area, *Oikos, 64*, 40-68, 1992.

Sigmundsson, F., Viscosity of the Earth beneath Iceland; comparison of model calculations with geological data (in Icelandic with English summary), M.Sc. thesis, 121 pp., University of Iceland, Reykjavík, 1990.

Sigmundsson, F., Postglacial rebound and asthenosphere viscosity in Iceland, *Geophys. Res. Lett., 18*, 1131-1134, 1991.

Sigmundsson, F., and P. Einarsson, Glacio-isostatic crustal movements caused by historical volume change of the Vatnajökull ice cap, Iceland, *Geophys. Res. Lett., 19*, 2123-2126, 1992.

Sigmundsson, F., P. Einarsson, and R. Bilham, Magma chamber deflation recorded by the Global Positioning System: The Hekla 1991 eruption, *Geophys. Res. Lett., 19*, 1483-1486, 1992a.

Sigmundsson, F., P. Einarsson, R. Bilham, and S. Sturkell, South Iceland 1992 GPS-measurements: Summary and daily observation logs, *Rep. 9201,* 19 pp., Nord. Volcanol. Inst., Reykjavík, Iceland, 1992b.

Sigmundsson, F., P. Einarsson, R. Bilham, and E. Sturkell, Rift-transform kinematics in south Iceland: Deformation from Global Positioning System measurements, 1986 to 1992, *J. Geophys. Res., 100*, 6235-6248, 1995.

Sturkell, E., F. Sigmundsson, P. Einarsson, and R. Bilham, Strain accumulation 1986-1992 across the Reykjanes Peninsula plate boundary, Iceland, determined from GPS measurements, *Geophys. Res. Lett., 21*, 125-128, 1994.

Thórarinsson, S., and G. E. Sigvaldason, The Hekla eruption of 1970, *Bull. Volcanol., 36*, 1-20, 1972a.

Thórarinsson, S., and G. E. Sigvaldason, The Tröllagígar eruption 1862-1864 (in Icelandic with English summary), *Jökull, 22*, 12-26, 1972b.

Thórdarson, Th., and S. Self, The Laki (Skaftár Fires) and Grímsvötn eruptions in 1783-1785, *Bull. Volcanol., 55*, 233-263, 1993.

Vogt, P. R., The Iceland phenomenon: Imprints of a hot spot on the ocean crust, and implications for flow below the plates, in *Geodynamics of Iceland and the North Atlantic Area,* 105-126 pp., edited by L. Kristjánsson, D. Reidel, Norwell, Mass., 1974.

Wendt, K., D. Möller, and B. Ritter, Geodetic measurements of surface deformations during the present rifting episode in NE Iceland, *J. Geophys. Res., 90*, 10,163-10,172, 1985.

Wessel, P., and W. H. F. Smith, New version of the generic mapping tools released, *EOS Trans. AGU, 76,* 329, 1995.

P. Einarsson, Science Institute, University of Iceland, Dunhaga 3, 107 Reykjavík, Iceland. (e-mail: palli@raunvis.hi.is)

S. Jónsson and F. Sigmundsson, Nordic Volcanological Institute, Grensásvegur 50, 108 Reykjavík, Iceland. (e-mail: fs@norvol.hi.is)

(Received February 21, 1996; revised December 4, 1996; accepted December 11, 1996.)